



Introduction to mesh based generated lumped parameter models for electromagnetic problems

Shuo Yang, Salim Asfirane, Sami Hlioui, Smail Mezani, Guillaume Krebs, Yacine Amara, Georges Barakat, Mohamed Gabsi, Wei Hua

► To cite this version:

Shuo Yang, Salim Asfirane, Sami Hlioui, Smail Mezani, Guillaume Krebs, et al.. Introduction to mesh based generated lumped parameter models for electromagnetic problems. CES transactions on electrical machines and systems, 2021, 5 (2), pp.152-162. 10.30941/CESTEMS.2021.00019 . hal-03840677

HAL Id: hal-03840677

<https://hal.science/hal-03840677>

Submitted on 2 Feb 2024

HAL is a multi-disciplinary open access archive for the deposit and dissemination of scientific research documents, whether they are published or not. The documents may come from teaching and research institutions in France or abroad, or from public or private research centers.

L'archive ouverte pluridisciplinaire **HAL**, est destinée au dépôt et à la diffusion de documents scientifiques de niveau recherche, publiés ou non, émanant des établissements d'enseignement et de recherche français ou étrangers, des laboratoires publics ou privés.

Introduction to Mesh Based Generated Lumped Parameter Models for Electromagnetic Problems

Shuo Yang, Salim Asfirane, Sami Hlioui, Smaïl Mezani, Guillaume Krebs, Yacine Amara, *Senior Member, IEEE*, Georges Barakat, Mohamed Gabsi and Wei Hua, *Senior Member IEEE*

Abstract—This paper is an introduction to mesh based generated reluctance network modeling. An overview of scientific works which led to the development of this approach is first presented. Basic concepts of the approach are then presented in the case of electromagnetic devices. A step-by-step procedure for coding the approach in the case of a flat linear permanent magnet machine is presented. Codes developed under MATLAB and Scilab environments are also included.

Index Terms—Lumped parameter modeling, finite element method, mesh, electromagnetic devices, modeling

I. INTRODUCTION

THE finite element method (FEM) is used in different engineering domains [1], and has proven to be very useful for the analysis and the design of engineering components and devices. Many commercial and open-source packages are now available and often used for teaching purposes and in R&D departments in industry [2]. It is inconceivable that an engineer can graduated without at least having heard about the FEM. Nevertheless, the FEM is always introduced at the end of engineering teaching programs, because it requires mastering relatively advanced mathematical concepts.

This isn't the case of lumped parameter models which require less mathematical knowledge, and which can be directly linked to the studied physical problems. This is why they are taught much earlier in the engineering teaching programs. They are qualified as semi-analytical approaches due to their derivation from simple analytical expressions, or as semi-numerical approaches because they require the discretization of the studied domains.

This contribution presents a tutorial introduction to mesh

based generation of lumped parameter models for electromagnetic problems. In the case of electromagnetic problems, the lumped parameter models are qualified as reluctance or permeance networks. In general, this approach is often developed with the minimum number of reluctances by identifying global flux tubes. Their identification is often done using FEM when the studied device is relatively complex, e.g., electrical machines.

The aim of the mesh based generated reluctance networks (MBGRN) approach is to avoid resorting to FEM and to make it an independent versatile tool, as FEM based software. This is done by automating the generation of these models, as it is the case in FEM.

Many recent works [3]–[12] have been dedicated to this approach, whether alone [3]–[8] or coupled with pure analytical models [8]–[12]. In [7], the software implementation of the approach is discussed and applied to a flux switching machine. The implementation was limited to the magnetic scalar potential formulation. In all cited references [3]–[12], the authors addressed one specific formulation. In [13], the authors coupled both magnetic scalar potential and mesh fluxes formulation, but didn't use the MBGRN. They used the classical approach based on the preliminary flux tubes identification method. In the present contribution, the goal is to discuss the fundamental bases of the approach, and it is presented for the two possible formulations: magnetic scalar potential, also known as the nodal approach, and the mesh fluxes formulation.

After positioning the approach regarding the works dedicated to the modeling of electromagnetic problems, and its genesis, basic concepts of the approach are presented. It is then detailed in the case of a flat linear permanent magnet machine. Codes developed under MATLAB and Scilab environments are provided along this contribution.

II. OVERVIEW OF THE GENESIS OF MBGRN

It is always difficult to identify the origin of a concept, because it may be proposed by several authors in different places with different names. In this section, an overview of the reluctance network models from its origin is proposed. It will help introduce the concept of MBGRN modeling.

The subject of this contribution is the modeling of electromagnetic devices. More precisely, it is the modeling of magnetic fields distribution, in these devices, which is targeted. In these objects, two domains should be distinguished:

Manuscript received April 19, 2020; revised August 26, 2020; accepted November 06, 2020. date of publication June 25, 2021; date of current version June 18, 2021.

Shuo Yang and Hua, Wei are with Southeast University, Nanjing, China.(e-mail: yangshuo9510@gmail.com; huawei1978@seu.edu.cn)

Salim Asfirane, Yacine Amara and Georges Barakat are with Université Le Havre Normandie. (e-mail:salim.asfirane@gmail.com; yacine.amara@univ-lehavre.fr; georges.barakat@univ-lehavre.fr)

Sami Hlioui is with Conservatoire national des arts et métiers(e-mail: sami.hlioui@lecnam.net)

Smaïl Mezani is with Université de Lorraine(e-mail: smail.mezani@univ-lorraine.fr)

Guillaume Krebs is with Université Paris-Saclay Faculté des Sciences d'Orsay(e-mail: Guillaume.Krebs@centralesupelec.fr)

Gabsi, Mohamed is with ENS Paris-Saclay(e-mail: Mohamed.gabsi@ens-paris-saclay.fr)

(Corresponding Author: Yacine Amara)

Digital Object Identifier 10.30941/CESTEMS.2021.00019

electricity and magnetism. Both domains are governed by the Maxwell's equations [14]. James Clerk Maxwell (1831–1879) mathematically formalized some works that have been done at that time by different scientists as André-Marie Ampère (1775–1836), Michael Faraday (1791–1867) and many others. While some scientists focused their works on the fundamental aspects related to electricity and magnetism, some others worked on the application of these fundamental aspects to electrical machines [15] [16].

Similarly to what has been done for electrical circuits, for which theoretical tools have been developed during the first half of the 19th century, some scientists, as John Hopkinson (1849–1898) and Gisbert Kapp (1852–1922), developed analog tools for the study of the magnetic circuits, during the second half of this century. An interesting historical overview on the genesis of the concept of magnetic circuit model can be found in [16].

The magnetic circuit model concept was the first to be used in order to compute the magnetic field distribution in electromagnetic devices. Numerical modeling tools, as the finite difference and the finite element methods, were only developed and used decades later [17]. With the development of numerical modeling approaches, the models used in physics and engineering were classified into two categories: analytical and numerical models. The magnetic circuit models, due to the fact that they are based on the use of spatially distributed reluctance (or permeance) elements, which are expressed analytically, overlap both modeling categories. They are qualified as semi-analytical or semi-numerical models. Many different terms are used to qualify the magnetic circuit model:

- 1) Magnetic circuits;
- 2) Magnetic equivalent circuits (MEC);
- 3) Reluctances or permeances networks (RN or PN);
- 4) Lumped parameter magnetic circuit models.

The term "lumped parameter model" is a general term used in different physical and related engineering domains. It reflects the spatial distribution of the circuit or network elements.

The generation of the RN can be done in two ways. The first way supposes the prior knowledge of the distribution of flux tubes, which are represented by the reluctance elements. The second approach, as for numerical modeling approaches, is based on a discretization of the studied domain without the prior knowledge of flux tubes distribution. Placed in the general context of solving Maxwell's equations, this idea is by no means new [18] [19]. Nevertheless, this contribution focuses on its application to magnetic circuits [20]–[28]. The development of these approaches requiring a more or less fine discretization in the space and time domains is concomitant with the development of computing science, and the larger availability of computing equipments (computers) [29]. This contribution is also motivated by the lack of commercial, or largely available, software tools based on this approach.

III. BASIC CONCEPTS OF THE MBGRN

Different concepts related to this approach, e.g. mesh type, elements type, are similar to corresponding concepts for FEM

[30]. In this contribution for the sake of simplicity and in order to simply introduce the approach, it will be described in the case of 2D problems (Cartesian coordinates) with a uniform homogeneous mesh, and rectangular elements (Fig. 1). Fig. 2 presents a flow chart of the MBGRN approach implementation. Being a numerical approach, this flow chart is similar to what could be found for the FEM approach.

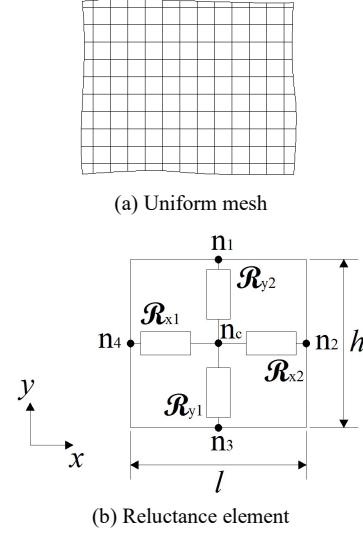


Fig. 1. Illustration of the MBGRN.

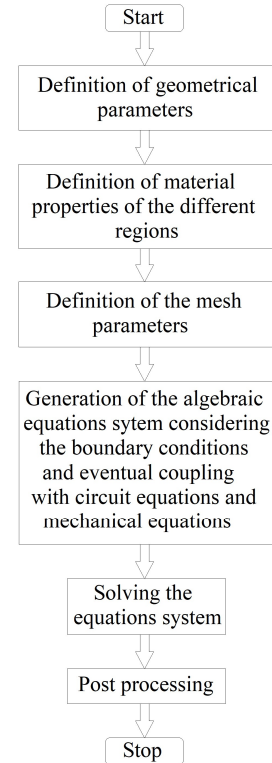


Fig. 2. Flow chart of the MBGRN modeling approach.

This flow chart can be adopted for the analysis of steady-state or transient problems. In electrical machines, the analysis of transient phenomenon requires the coupling of the MBGRN to electrical circuits and mechanical equations. Aiming at introducing the MBGRN approach, its coupling with electric circuits and mechanical equations are not discussed.

Nevertheless, being equivalent from a conceptual point of view to FEM approach, interested readers could consult references [30], [31] and [32].

This approach is based on the subdivision of the studied domain into a certain number of reluctance elements (Fig. 1). Each element is composed of one central node and 4 nodes at the element boundary. The central node is connected to the boundary nodes via 4 reluctances [Fig. 1(b)]. The expressions of the four reluctances composing the reluctance element are given by:

$$\mathcal{R}_{x1} = \mathcal{R}_{x2} = \frac{1}{\mu_0 \mu_r} \frac{l}{2l_a h}, \text{ and } \mathcal{R}_{y1} = \mathcal{R}_{y2} = \frac{1}{\mu_0 \mu_r} \frac{h}{2l_a l}, \quad (1)$$

where, l and h are the length and the height of the element [Fig. 1(b)], μ_0 and μ_r are the permeability of the vacuum and the relative permeability of the region (material) where the element is located, and finally, l_a is the active length of modeled problem.

Note that the use of triangular elements is also possible [8] [33]. For the sake of simplicity, the MBGRN approach will be implemented in the case of a linear structure, where the geometry is well adapted for rectangular elements. In case the geometry imposes it [33], the triangular elements could be adopted exclusively or along with the rectangular ones.

In following subsections, all elements required to build the algebraic equations system to solve in order to obtain the magnetic field distribution for the studied device are presented.

A. Mesh and Elements Numbering

In order to simply introduce the approach, a uniform homogenous mesh, only containing rectangular elements, is adopted [Fig. 1(a)]. The 2D studied domain is a rectangular area. It is divided into m elements (segments) in x direction and n elements (segments) in y direction. Fig. 3 illustrates the way the elements of this mesh are indexed. In order to identify the number of an element in relation to its position in the mesh a matrix representation is adopted (2). Two vectors, one corresponding to the position of the element in x direction (\mathbf{s} vector) and the other to its position in y direction (\mathbf{r} vector), are adopted. This matrix is given by:

$$MN = \begin{bmatrix} (1,1) & (1,2) & \cdots & (1,m-1) & (1,m) \\ (2,1) & (2,2) & \cdots & (2,m-1) & (2,m) \\ \vdots & \vdots & & \vdots & \vdots \\ (r,s) & & & & \\ \vdots & \vdots & & \vdots & \vdots \\ (n,1) & (n,2) & \cdots & (n,m-1) & (n,m) \end{bmatrix}. \quad (2)$$

The number (index) of an element (en) located at the position (r,s) in the matrix is then given by:

$$en = (r-1) \cdot m + s. \quad (3)$$

Apart from the elements located at the boundaries of the studied domain, an element number en will be connected to four elements as shown in Fig. 3. Treatment of elements at the boundaries is analyzed in following subsection.

B. Boundary Conditions Consideration

Four different boundary conditions could be encountered:

- 1) Parallel magnetic field boundary condition;
- 2) Normal magnetic field boundary condition;
- 3) Cyclic (or periodic) boundary conditions;
- 4) Anti-cyclic (or anti-periodic) boundary conditions.

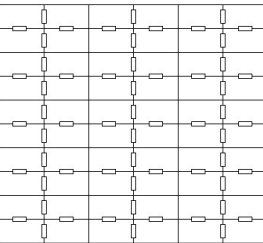
(n-1)m+1	(n-1)m+2		nm-1	nm
(n-2)m+1	(n-2)m+2		(n-1)m-1	(n-1)m
				
m+1	m+2		2m-1	2m
1	2		m-1	m

Fig. 3. Indexing of the mesh elements.

Fig. 4 illustrates how the parallel magnetic field boundary condition impacts the reluctance elements located at this boundary. Reluctances connected to this boundary are set equal to the infinite. This means that no magnetic flux is going out from this boundary. Fig. 5 illustrates how the normal magnetic field boundary condition is considered in the RN. If the magnetic field is considered deriving from a scalar magnetic potential U , its components, in a 2D Cartesian coordinates referential, can be obtained from

$$\vec{H} = -\vec{grad}U = -\frac{\partial U}{\partial x} \vec{e}_x - \frac{\partial U}{\partial y} \vec{e}_y. \quad (4)$$

A normal magnetic field boundary condition applied to a line located at a given y coordinates, as the example in Fig. 4, is equivalent to imposing a constant value of the scalar magnetic potential U to nodes located on this line. This constant value could be set null.

For the periodic or the anti-periodic boundary conditions, two boundaries are concerned. As for the FEM, these boundaries should be meshed similarly. Considering that these two boundaries are located at positions $x = 0$ m and $x = L_t$, where L_t is the total length of the studied domain in x direction. Fig. 6 shows an illustration of the way these two boundary conditions are treated for two elements i and $(i+m-1)$ located at the two boundaries respectively.

If the periodic boundary condition is applied at the two boundaries, the equation related to the element i , $(i+m-1)$ respectively, is established by considering that the element connected to it at the left-hand side, right-hand side respectively, is the element $(i+m-1)$, i respectively.

This corresponds to considering that the magnetic flux incoming from the left-hand side of element i , is equal to the flux outgoing in right direction from the element $(i+m-1)$.

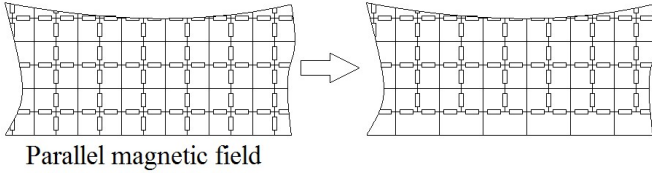


Fig. 4. Parallel magnetic field boundary condition.

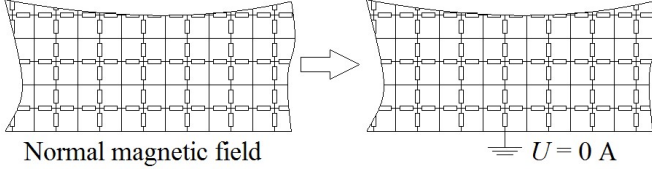


Fig. 5. Normal magnetic field boundary condition.

If the anti-periodic condition is applied at the two boundaries, the equation related to element i , $(i+m-1)$ respectively, is established by considering that the element connected to it at the left-hand side, right-hand side respectively, has a value of U , at its central node, which is opposite to the value of U in the element $(i+m-1)$, i respectively. The use of the sign minus in the numbers of the elements in Fig. 6(b) is intended to highlight this aspect. The antiperiodic boundary conditions also correspond to consider that the magnetic flux incoming from the left-hand side of the element i is opposite to the flux outgoing toward right direction from the element $(i+m-1)$.

C. Magnetic Field Sources Modeling

Two magnetic field sources do exist in electrical machines: coils or windings, and permanent magnets (PM). Permanent magnets can either be modeled by a flux source in parallel with a reluctance or a magneto-motive force MMF in series with a reluctance, as shown in Fig. 7.

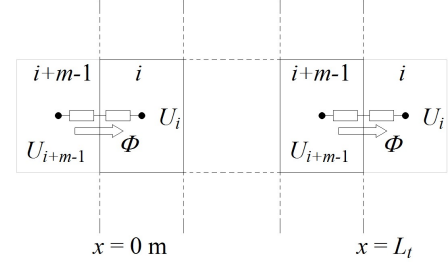
MMF sources corresponding to a winding have not necessarily to be represented within the RN. They have to when magnetic scalar potential at central nodes are chosen as the unknowns. In this case, Fig. 8 shows the variation of MMF with the coordinates corresponding to the direction for which the coil closes (x direction). This figure shows the modelling principle on the illustrative example of the following section. w_s and τ_s are respectively the slot opening and the slot pitch.

MMF sources are located in the branches perpendicular to the direction for which the coil closes (x direction). All MMF sources are located between y_0 and $y_0 + h_s$, where h_s is the slot height. The first slot ($x \in [x_0, x_0 + w_s]$) is divided into two elements in x direction. The values of the MMF sources in the elements, located between x_0 and $x_0 + w_s/2$, will correspond to $\text{MMF}(x_0 + w_s/4)/N_{sy}/2$, where N_{sy} is the number of elements in the slot in y direction (two elements in the case of Fig. 8). Notice that $x_0 + w_s/4$ is the coordinate of the central nodes of these elements in x direction. The total MMF is obtained by summing MMF of the different phases.

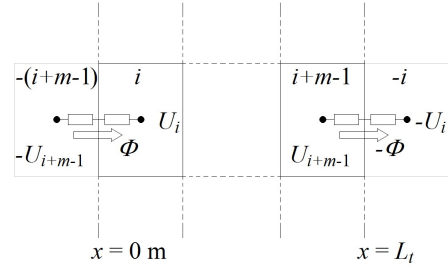
If the mesh fluxes are chosen as the unknowns, the MMF sources haven't to be considered in the RN. The MMF sources are naturally considered by the Ampere's law, which is the basic law helping establishing the algebraic equations system. Further details are provided in subsection III.E.

D. Magnetic Scalar Potential Formulation (MSPF)

In this formulation, the unknowns are the magnetic scalar potentials at each central node of the reluctance elements. The so-called nodal method [34] is used to generate the algebraic equations system.

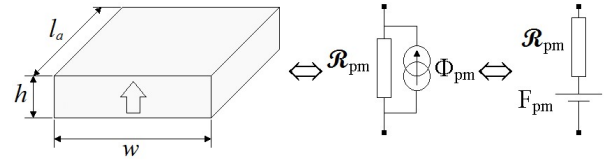


(a) Cyclic boundary conditions



(b) Anti-cyclic boundary conditions

Fig. 6. Periodic and anti-periodic boundary conditions illustration.



$$\begin{cases} \mathcal{R}_{pm} = \frac{1}{\mu_0 \mu_{rpm}} \frac{h}{l_a w} \\ \Phi_{pm} = B_r l w \\ F_{pm} = \frac{B_r}{\mu_0 \mu_{rpm}} h \end{cases}$$

Fig. 7. Permanent magnet (PM) region modeling.

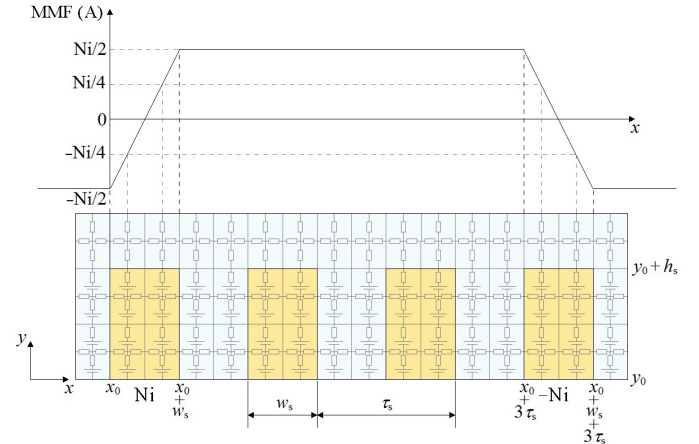


Fig. 8. Windings MMF distribution.

Fig. 9 illustrates how the equations corresponding to a node i are determined after Kirchhoff's laws. According to Kirchhoff's laws, it can be established that

$$\sum_{\substack{j=1 \\ j \neq i}}^{nn} \Phi_{ij} = 0 \quad \text{Wb} \quad \text{and} \quad U_i - U_j = Fms_{ij} - \frac{(\Phi_{ij} - \Phi_{s_{ij}})}{P_{ij}} \quad (5)$$

and then,

$$\left(\sum_{\substack{j=1 \\ j \neq i}}^{nn} P_{ij} \right) \cdot U_i + \sum_{\substack{j=1 \\ j \neq i}}^{nn} (-P_{ij}) \cdot U_j = \sum_{\substack{j=1 \\ j \neq i}}^{nn} (\Phi_{s_{ij}} + P_{ij} \cdot Fms_{ij}) \quad (6)$$

The equations system, corresponding to the RN, is expressed using matrix formulation as

$$[P][U] = [\Phi] \quad (7)$$

where $[P]$ $[n \cdot m \times n \cdot m]$ is the permeance matrix, $[U]$ $[n \cdot m \times 1]$ is the magnetic scalar potential vector (the unknowns vector), and $[\Phi]$ $[n \cdot m \times 1]$ is the flux sources vector. $nn = n \cdot m$ is the number of nodes. Having adopted a uniform homogenous mesh, the maximum number of non-null elements in a given line of the matrix $[P]$ is 5. The matrix is then sparse.

E. Mesh Fluxes Formulation (MFF)

In this formulation, the unknowns are the mesh fluxes. The so-called mesh method [34] is used to generate the algebraic equations system. Fig. 10 illustrates how the equations corresponding to a mesh i are determined from Kirchhoff's and Ampere's laws. According to these laws, it can be established that

$$\oint_{ABCD} \vec{H} d\vec{l} = \left[\begin{array}{l} \mathcal{R}_{AB}(\Phi_i - \Phi_{i-m}) + \mathcal{R}_{BC}(\Phi_i - \Phi_{i+1}) \\ + \mathcal{R}_{CD}(\Phi_i - \Phi_{i+m}) + \mathcal{R}_{DA}(\Phi_i - \Phi_{i-1}) \end{array} \right] = Ni, \quad (8)$$

where Ni is the number of Ampere-turns (MMF) surrounded by the mesh loop. Ni is counted positive if the current is coming out of the plan towards reader, and negative inversely.

The equations system, corresponding to the RN when mesh fluxes are chosen as the unknowns, is expressed using matrix formulation as

$$[R][\Phi] = [F], \quad (9)$$

where $[R]$ is the reluctance matrix, $[\Phi]$ is the mesh fluxes vector (the unknowns vector), and $[F]$ is the magneto-motive forces vector. Depending on the boundary conditions the number of unknowns, problem dimension, in this formulation could be lower or higher as compared to previous formulation. Having adopted a uniform homogenous mesh, the maximum number of non-null elements in a given line of the matrix $[R]$ is 5. The matrix is then also sparse.

F. Motion Consideration

Techniques used for the consideration of motion in FEM [30] can be simply adapted to the MBGRN approach. In the illustrative example presented in the next section, the moving armature is non-salient. The stator armature is salient considering the slotting effect. The motion consideration is simply realized by modifying the right-hand side excitation vector, $[\Phi]$ or $[F]$, in (7) or (9), respectively. No need to actualize elements values of matrices $[P]$ or $[R]$. This is specific to the chosen example.

As for FEM, the motion can be considered by remeshing the air-gap region [30] [35], using sliding surface between the moving region and the static one [30], and others [36].

G. Magnetic Saturation Consideration

If magnetic saturation is considered, the algebraic equations system becomes non-linear (10). It can only be solved using iterative approaches. The main approaches used for that purpose are the Newton method and fixed point method [30].

$$\begin{cases} [P(U)][U] = [\Phi(U)] & \text{for MSPF} \\ [R(\Phi)][\Phi] = [F] & \text{for MFF} \end{cases} \quad (10)$$

As illustrated by (10), the consideration of magnetic saturation will result in the dependence of matrix $[P]$, and vector $[\Phi]$, on the solution vector $[U]$, for the MSPF, while only the matrix $[R]$ will depend on the solution vector $[\Phi]$, for the MFF. It is then easier to adopt the MFF when considering the magnetic saturation. Authors in [34] have highlighted the superiority of the MFF as compared to MSPF, when magnetic saturation is considered.

In following section, the magnetic saturation is considered using the MFF, and the fixed point method is used in order to solve the non-linear algebraic equations system (Fig. 11).

The convergence criterion is given by:

$$\varepsilon = \sqrt{\frac{\sum_{i=1}^{n \cdot m} (\Phi_i^{k+1} - \Phi_i^k)^2}{\sum_{i=1}^{n \cdot m} (\Phi_i^{k+1})^2}} < 10^{-3}, \quad (11)$$

where k refers to the iteration number. If the number of iterations exceeds a certain number Nb_I , the resolution is stopped, even if the convergence criterion is not reached.

Fig. 11 shows the adopted algorithm for solving the non-linear algebraic equations system. Initial solution is obtained considering the value of relative permeability of iron core at the origin.

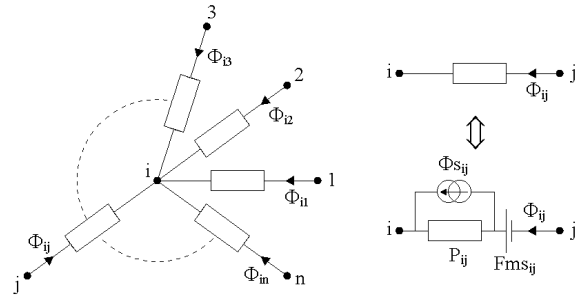


Fig. 9. Equation setting for the i^{th} node.

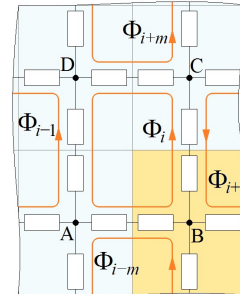


Fig. 10. Equation setting for the i^{th} mesh.

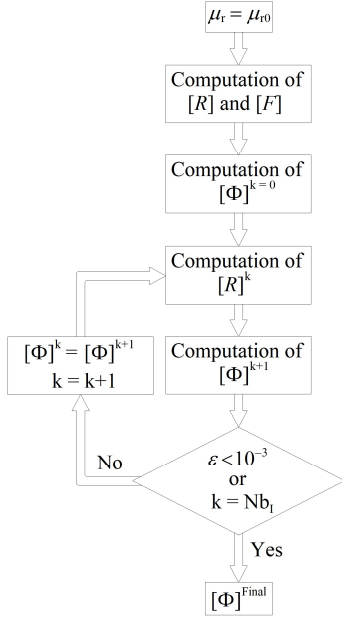


Fig. 11. Non-linear algebraic equations system solving algorithm.

IV. ILLUSTRATIVE EXAMPLE

The MBGRN is implemented in the case of a flat linear permanent magnet machine (FLPM) (Fig. 12). The MBGRN approach is compared to FEM in the cases of linear and non-linear iron cores characteristics. In the linear case, the two precedent formulations are used, and compared to corresponding analyses using the FEM. In the non-linear case (consideration of magnetic saturation), only the MFF MBGRN is compared to the FEM.

Due to geometric and electromagnetic symmetries; only one pole pitch is modeled. Anti-periodic boundary conditions are adopted. Table I gives main machine's dimensions. Equation (12) gives the non-linear characteristic of iron cores used in both the FEM and the MFF MBGRN.

TABLE I
MACHINE CHARACTERISTICS

Mechanical air-gap e (mm)	1
Pole pitch τ_p (mm)	60
$h_{st}, h_s, h_m, h_{mbi}, \tau_m, \tau_s$ and w_s (mm)	30, 20, 10, 10, 55, 20, 10
Active length (mm)	1000
PM magnetic remanence B_r (T)	1.2
Relative permeability of iron μ_{ri} and PM μ_{rm}	7500, 1

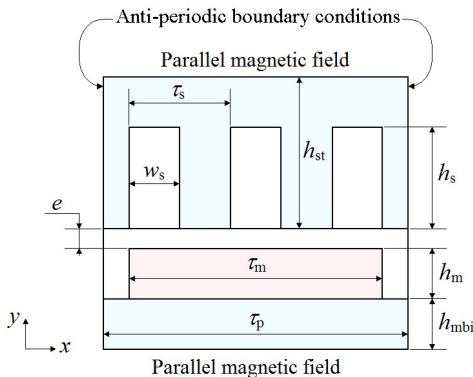
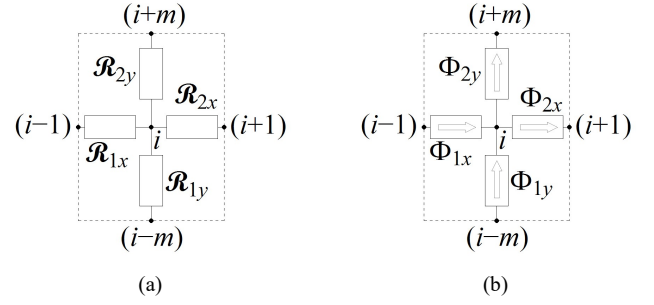


Fig. 12. Longitudinal cross-sectional view of the studied FLPM structure.

Fig. 13. Computation of magnetic field \mathbf{B} components for node i .

$$\mu_r(H) = 1 + \left(\frac{2 \cdot B_{sat}}{\mu_0 \cdot \pi \cdot H} \right) \cdot \arctan \left(\frac{\pi \cdot (\mu_{r0} - 1) \cdot \mu_0 \cdot H}{2 \cdot B_{sat}} \right) \quad (12)$$

B_{sat} is the saturation induction, set equal to 1.99, and μ_{r0} is the value of relative permeability at the origin, set equal to 7500.

Programs coded under MATLAB and Scilab environments allowing the analyses can be downloaded from [37] for the linear case, and from [38] for the non-linear case. They are coded using simple instructions.

A. Computation of Local Quantities

The magnetic field \mathbf{B} components at the central node of an element i (Fig. 13) are computed by

$$\begin{cases} B_{ix} = \frac{1}{2} \cdot \left(\frac{U_{i-1} - U_i}{\mathcal{R}_{1x}} + \frac{U_i - U_{i+1}}{\mathcal{R}_{2x}} \right) = \frac{1}{2} \cdot \left(\frac{\Phi_{1x}}{l_a h} + \frac{\Phi_{2x}}{l_a h} \right) \\ B_{iy} = \frac{1}{2} \cdot \left(\frac{U_{i-m} - U_i}{\mathcal{R}_{1y}} + \frac{U_i - U_{i+m}}{\mathcal{R}_{2y}} \right) = \frac{1}{2} \cdot \left(\frac{\Phi_{1y}}{l_a l} + \frac{\Phi_{2y}}{l_a l} \right) \end{cases} \quad (13)$$

Fig. 13 shows the different quantities used in (13). The local quantities are used to compute global quantities.

B. Computation of Global Quantities

The global quantities are computed in a post-processing phase, as it is done in FEM packages. The phase flux linkages, under open-circuit or load conditions, are computed by summing fluxes in the RN branches located at mid-height of the slots, and spanning one pole pitch, which corresponds to the opening distance of a phase coil for the studied machine. Fig. 14 illustrates how this is done for the used model which is limited to one pole pitch. The total flux in this coil is given by

$$\Phi_t = \Phi_0 - \Phi_1 \quad (14)$$

The voltage (EMF under open-circuit condition) is computed by differentiating the total flux and multiplying it to the number of turns.

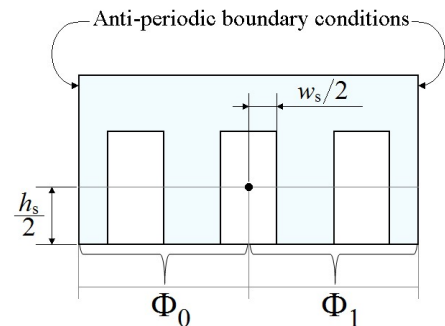


Fig. 14. Computation of the total flux in a coil spanning one pole pitch.

The cogging force under open-circuit condition or the thrust force under load conditions are computed using the Maxwell stress tensor (MST). MST can also be used to compute the attraction force between the stator and moving armature. The force components in x and y directions are given by

$$F_x = \frac{l_a}{\mu_0} \int_0^{\tau_p} B_y B_x dx, \text{ and } F_y = \frac{l_a}{2\mu_0} \int_0^{\tau_p} (B_y^2 - B_x^2) dx \quad (15)$$

B_x and B_y correspond to the components of magnetic field vector \mathbf{B} in nodes located at a given y coordinate in the air-gap. As for FEM, the mesh of the air-gap should be given a particular attention in order to insure good quality results.

Other global quantities as the iron losses can also be computed in the post-processing phase [39]. Nevertheless, as an introduction to the MBGRN, the computation of the global quantities is limited to the voltages and the forces.

C. Comparison with FEM

Since results from MBGRN approach using magnetic scalar potential and mesh fluxes formulations are identical, in the linear case, only these issued from the second are presented. The results are plotted for a mesh with $m = 120$ and $n = 102$, which corresponds to 12240 square elements. By doing so, the air-gap contains two layers of elements. It is referred to results from the MBGRN in following figures by simply using the acronym RN. FLUX2D package [2] is used for the FEM computations.

Fig. 15 compares magnetic field \mathbf{B} components under open-circuit condition. The position for which these spatial distributions are plotted corresponds to the one of Fig. 12, the PM having a positive magnetization. The origin point ($x = 0$ m, $y = 0$ m) corresponds to the bottom-left corner of the structure. The spatial distributions are plotted for a path located at $y = h_{mbi} + h_m + 3e/4$, which corresponds to $r = 42$. The slotting effect is clearly visible in this figure.

Fig. 16(a) shows the variation of cogging force (CF). The CF period corresponds to τ_s . The moving armature is moving toward negative x values. Fig. 16(b) shows the phase electromotive force (EMF) per turn, for one pole pair, for a linear speed $v = 1$ m/s.

Fig. 17(a) compares magnetic field \mathbf{B} components only due to armature reaction field (ARF) (no PM). Fig. 17(b) shows in which conditions these spatial distributions are obtained. Fig. 18(a) shows the variation of thrust force (TF), for one pole pair, with the displacement x_d . The current in each phase is imposed with a null phase shift with the corresponding phase EMF (Maximum force per-Ampere (MFPA) control). The maximum current density is set equal to 5 A/mm². Fig. 18(b) shows the phase voltage per turn, for one pole pair.

Same comparisons are performed in the non-linear case. These comparisons are shown in Figs. 19 to 22. In this case, discrepancies appear between results obtained from the FEM and the MFF MBGRN. Table II gives relative errors between both methods, considering the FEM as the reference. The errors are relatively low.

From all these comparisons, it can be concluded that the MBGRN approach performs similarly to what can be done using FEM.

TABLE II
RELATIVE ERROR IN NON-LINEAR CASE

Quantity	Relative error (%)
Cogging force (RMS value) [Fig. 21(a)]	3.12
EMF (RMS value) [Fig. 21(b)]	3.96
Thrust force (Mean value) [Fig. 22(a)]	3.11
Thrust force (RMS value) [Fig. 22(a)]	2.42
Voltage (RMS value) [Fig. 22(b)]	3.76

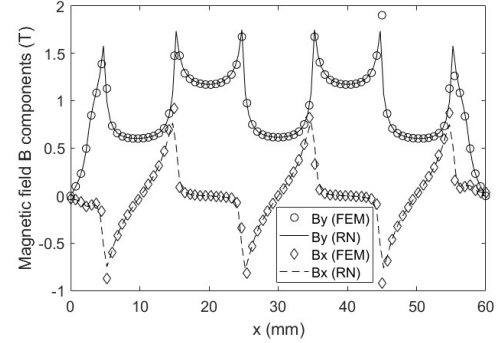
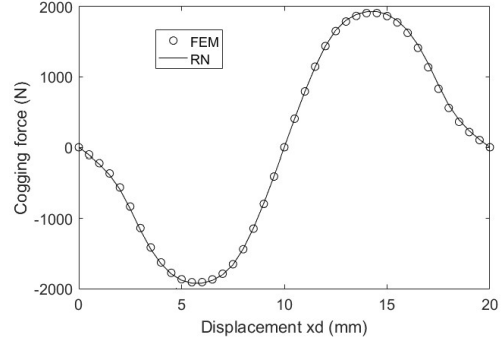
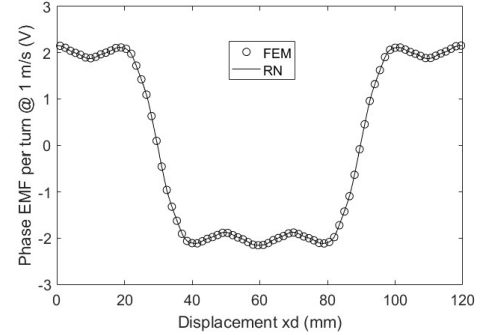


Fig. 15. Magnetic field \mathbf{B} components in the air-gap (open-circuit condition).

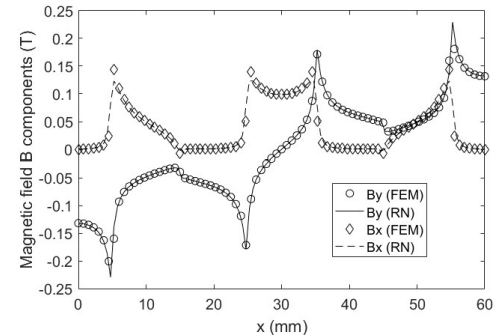


(a) Cogging force

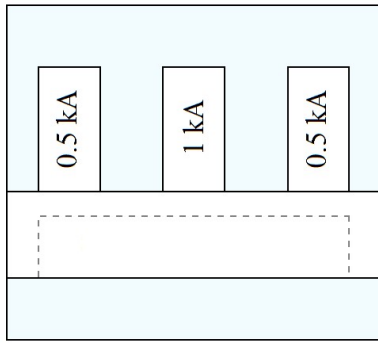


(b) EMF for a linear speed $v = 1$ m/s

Fig. 16. Global quantities under open-circuit condition.



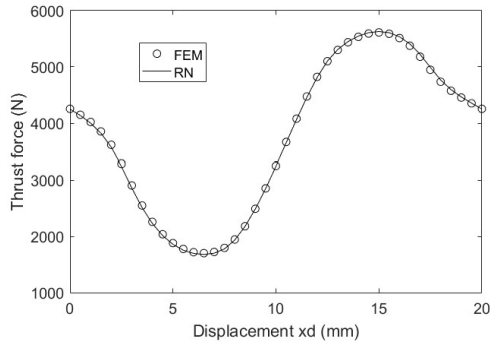
(a) Magnetic field \mathbf{B} components in the air-gap (armature field reaction).



(b) Illustration of the conditions of computation of the ARF.

Fig. 17. Comparison of ARF magnetic field components.

Along with this contribution, these programs can be used in classrooms for the introduction of electromagnetic devices design and analysis.



(a) Thrust force

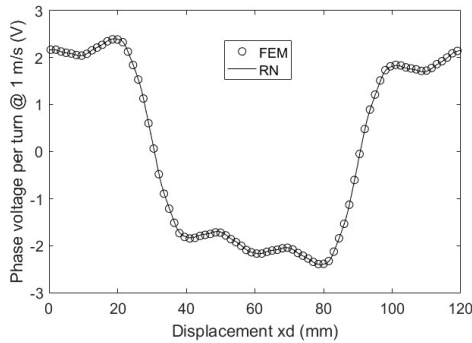

 (b) Phase voltage under load condition for a linear speed $v = 1$ m/s

Fig. 18. Global quantities under load condition.

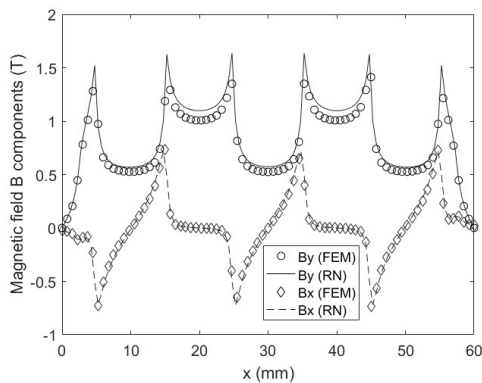


Fig. 19. Magnetic field B components in the air-gap (open-circuit condition).

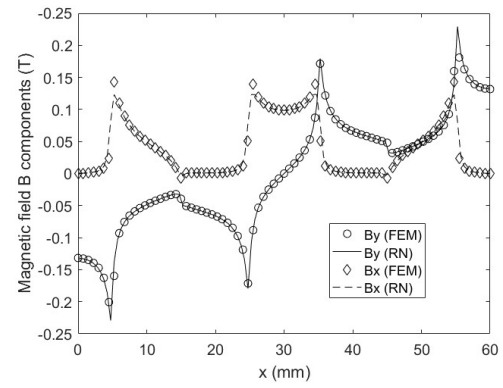
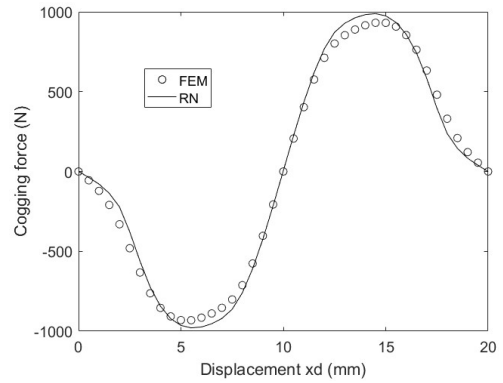


Fig. 20. Magnetic field B components in the air-gap (armature field reaction).



(a) Cogging force

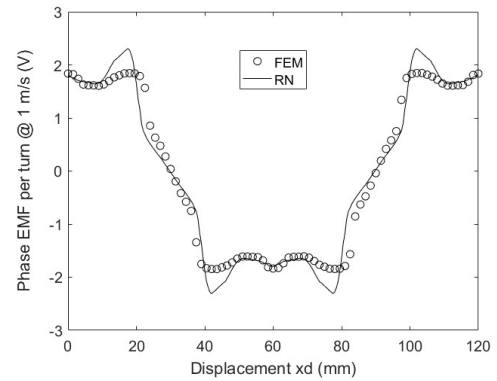
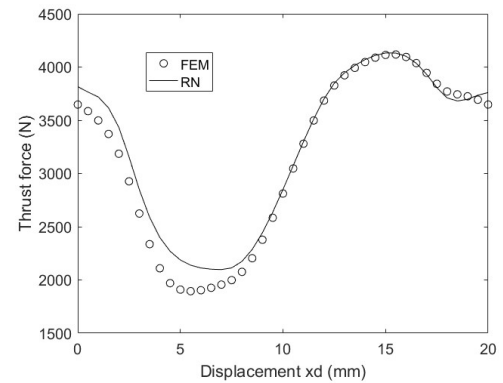
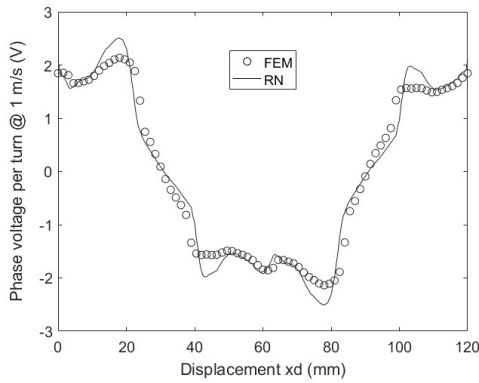

 (b) EMF for a linear speed $v = 1$ m/s

Fig. 21. Global quantities under open-circuit condition.



(a) Thrust force



(b) Phase voltage under load condition for a linear speed $v = 1$ m/s

Fig. 22. Global quantities under load condition.

V. CONCLUSIONS

An introduction to the MBGRN approach has been presented. This approach requires less mathematical knowledge as compared to FEM, and may be adapted to also study other physics involved in the operation of a device. For example, by replacing the reluctances by thermal resistances, this approach can help study the thermal behavior.

The provided programs have been coded under MATLAB and Scilab environments, which are widely distributed and used in the academic institutions. Very simple instructions have been used to make them the most simple to understand.

This approach, introduced in the case of 2D problems, can also be used for 3D problems [5] [40]. Its introduction for 3D problems will be the subject of a future contribution.

REFERENCES

- [1] M. N. O. Sadiku, "A simple introduction to finite element analysis of electromagnetic problems," *IEEE Trans. Educ.*, vol. E-29, no. 2, pp. 85–93, May 1989. DOI: 10.1109/13.28037.
- [2] A. Foggia, J.-L. Coulomb, G. Reyne, F. Ossart, and A. Kedous-Lebouc, "The French experience in integrating the program FLUX2D in the undergraduate curriculum at the Institut National Polytechnique de Grenoble," *IEEE Trans. Educ.*, vol. 36, no. 2, pp. 85–93, May 1993. DOI: 10.1109/13.214713.
- [3] M.-F. Hsieh and Y.-C. Hsu, "A generalized magnetic circuit modeling approach for design of surface permanent-magnet machines," *IEEE Trans. Ind. Electron.*, vol. 59, no. 2, pp. 779–792, Feb. 2012.
- [4] G. Liu, L. Ding, W. Zhao, Q. Chen, and S. Jiang, "Nonlinear equivalent magnetic network of a linear permanent magnet Vernier machine with end effect consideration," *IEEE Trans. Magn.*, vol. 54, no. 1, paper 8100209, January 2018. DOI: 10.1109/TMAG.2017.2751551
- [5] S. Asfrane, S. Hlioui, Y. Amara and M. Gabsi, "Study of a hybrid excitation synchronous machine: modeling and experimental validation," *Math. Comput. Appl.*, 2019, 24, 34; doi:10.3390/mca24020034
- [6] D. Cao, W. Zhao, J. Ji, L. Ding, and J. Zheng, "A generalized equivalent magnetic network modeling method for vehicular dual-permanent-magnet Vernier machines," *IEEE Trans. Energy Convers.*, vol. 34, no. 4, pp. 1950–1962, Dec. 2019. DOI: 10.1109/TEC.2019.2921699
- [7] S. Yang, Y. Amara, W. Hua, and G. Barakat, "Development of a generic framework for lumped parameter modeling," *Open Physics*, vol. 18, pp. 365–373, 2020. DOI: <https://doi.org/10.1515/phys-2020-0168>
- [8] S. Ouagued, Y. Amara, and G. Barakat, "Comparison of hybrid analytical modelling and reluctance network modelling for pre-design purposes," *Mathematics and Computers in Simulation*, vol. 130, pp. 3–21, Dec. 2016. <https://doi.org/10.1016/j.matcom.2016.05.001>
- [9] A. Hemeida and P. Sergeant, "Analytical modeling of surface PMSM using a combined solution of Maxwell's equations and magnetic equivalent circuit," *IEEE Trans. Magn.*, vol. 50, no. 12, paper 7027913, Dec. 2014. DOI: 10.1109/TMAG.2014.2330801
- [10] K. J. W. Pluk, J. W. Jansen, and E. A. Lomonova, "Hybrid analytical modeling: Fourier modeling combined with mesh-based magnetic equivalent circuits," *IEEE Trans. Magn.*, vol. 51, no. 8, paper 8106812, August 2015. DOI: 10.1109/TMAG.2015.2419197
- [11] K. J. W. Pluk, J. W. Jansen, and E. A. Lomonova, "3-D hybrid analytical modeling: 3-D Fourier modeling combined with mesh-based 3-D magnetic equivalent circuits," *IEEE Trans. Magn.*, vol. 51, no. 12, paper 8208614, Dec. 2015. DOI: 10.1109/TMAG.2015.2455951
- [12] D. Ceylan, L. A. J. Friedrich, K. O. Boynov, and E. A. Lomonova, "Convergence analysis of the fixed-point method with the hybrid analytical modeling for 2-D nonlinear magnetostatic problems," *IEEE Trans. Magn.*, Early Access, 2020. DOI: 10.1109/TMAG.2020.3024539
- [13] A. Mahyob, P. Reghem, and G. Barakat, "Permeance network modeling of the stator winding faults in electrical machines," *IEEE Trans. Magn.*, vol. 45, no. 3, pp. 1820–1823, March 2009. DOI: 10.1109/TMAG.2009.2012780
- [14] James Clerk Maxwell, *A Treatise on Electricity and Magnetism*, in two volumes, Clarendon Press Series, Oxford, U.K., 1873.
- [15] Romuald-Victor Picou, *Traité théorique et pratique des machines dynamo-électriques*, Librairie Polytechnique, Baudry et Cie, Paris, France, 1889.
- [16] D. W. Jordan, "The magnetic circuit model, 1850-1890: The resisted flow image in magnetostatics," *Br. J. Hist. Sci.*, vol. 23, no. 2, pp. 131–173, June 1990. doi:10.1017/S0007087400044733
- [17] C. W. Trowbridge and J. K. Sykulski, "Establishing a web based archive of papers in computational electromagnetics," Conference Record, Compumag Sydney, July 2011.
- [18] G. Kron, "Numerical solution of ordinary and partial differential equations by means of equivalent circuits," *J. Appl. Phys.*, vol. 16, pp. 172–186, Mar. 1945. doi: 10.1063/1.1707568
- [19] W. R. Zimmerman, "Network analogs of Maxwell's field equations in one and two dimensions," *IEEE Trans. Educ.*, vol. E-25, no. 1, pp. 4–9, Feb. 1982. DOI: 10.1109/TE.1982.4321523
- [20] E. I. King, "Equivalent circuits for two-dimensional magnetic fields: 1-The static field," *IEEE Trans. Power App. Syst.*, Vol. PAS-85, No. 9, pp. 927–935, September, 1966. DOI: 10.1109/TPAS.1966.291715
- [21] C. J. Carpenter, "Finite element network models and their application to eddy-current problems," *Proc. Inst. Elect. Eng.*, vol. 122, pp. 455–461, Apr. 1975. DOI: 10.1049/piee.1975.0125
- [22] J. Turowski, M. Turowski, and M. Kopec, "Method of three-dimensional network solution of leakage field of three-phase transformers," *IEEE Trans. Magn.*, vol. 26, no. 5, pp. 2911–2919, Sept. 1990. DOI: 10.1109/20.104906
- [23] J. Worotynski, M. Turowski, and E. Worotynska, "Generation of an optimal reluctance network model for fast 2-D and 3-D simulations of electromagnetic devices," in *Proc. 2nd Int. Conf. Comput. Electromagn.*, London, U.K., Apr. 1994, pp. 116–119.
- [24] J. Sykulski et al., *Computational Magnetism*, London, U.K.: Chapman & Hall, 1995.
- [25] C. B. Rasmussen and E. Ritchie, "A magnetic equivalent circuit approach for predicting PM motor performance," in *Proc. 32nd IAS Annu. Meeting Conf. Rec. IEEE Ind. Appl.*, vol. 1, New Orleans, LA, USA, Oct. 1997, pp. 10–17. DOI: 10.1109/IAS.1997.643001
- [26] A. Demenko, L. Nowak, and W. Szlag, "Reluctance network formed by means of edge element method," *IEEE Trans. Magn.*, vol. 34, no. 5, pp. 2485–2488, Sept. 1998. DOI: 10.1109/20.717572
- [27] J. Perho, *Reluctance network for analysing induction machines*, Ph.D. Thesis, *Acta Polytech. Scand., Electr. Eng. Ser.*, vol. 110, Dec. 2002.
- [28] A. Delale, L. Albert, L. Gerbaud, and F. Wurtz, "Automatic generation of sizing models for the optimization of electromagnetic devices using reluctance networks," *IEEE Trans. Magn.*, vol. 40, no. 2, pp. 830–833, March 2004. DOI: 10.1109/TMAG.2004.824908
- [29] Alexander Kusko and Theodor Wroblewski, *Computer-aided design of magnetic circuits*, USA: The MIT Press, 1969.

- [30] G. Meunier, *The Finite Element Method for Electromagnetic Modeling*, London, U.K.: ISTE Ltd., 2008. [Online]. Available @: <http://www.iste.co.uk/book.php?id=168>
- [31] V. Ostovic, *Dynamics of Saturated Electric Machines*, Springer-Verlag New York Inc., 1989.
- [32] H. Roisse, M. Hecquet, and P. Brochet, "Simulation of synchronous machines using an electric-magnetic coupled network model," *IEEE Trans. Magn.*, vol. 34, no. 5, pp. 3656–3659, Sept. 1998. DOI: 10.1109/20.717864
- [33] S. Ouagued, Y. Amara, and G. Barakat, "Cogging force analysis of linear permanent magnet machines using a hybrid analytical model," *IEEE Trans. Magn.*, vol. 52, no. 7, paper 8202704, July 2016. DOI: 10.1109/TMAG.2016.2521825
- [34] H. W. Derbas, J. M. Williams, A. C. Koenig, and S. D. Pekarek, "A comparison of nodal- and mesh-based magnetic equivalent circuit models," *IEEE Trans. Energy Convers.*, vol. 24, no. 2, pp. 388–396, Jun. 2009. DOI: 10.1109/TEC.2008.2002037
- [35] M. L. Bash, J. M. Williams, and S. D. Pekarek, "Incorporating motion in mesh-based magnetic equivalent circuits," *IEEE Trans. Energy Convers.*, vol. 25, no. 2, pp. 329–338, Jun. 2010. DOI: 10.1109/TEC.2009.2035513
- [36] M. A. Benhamida, H. Ennassiri, Y. Amara, G. Barakat, and N. Debbah, "Study of switching flux permanent magnet machines using interpolation based reluctance network model," in *Proc. Int. Conf. Elect. Sci. Technol. Maghreb (CISTEM)*, Marrakech, Morocco, 2016, pp. 1–7. DOI: 10.1109/CISTEM.2016.8066809
- [37] <https://1drv.ms/u/s!AogSAGtYvycUimFy-CvOpeWaKv4J?e=6MNFFI>
- [38] <https://1drv.ms/u/s!AogSAGtYvycUimcf7Zwe27GA2g3J?e=YyaU1k>
- [39] S. Asfirane, S. Hlioui, Y. Amara, O. De La Barriere, G. Barakat, and M. Gabsi, "Global quantities computation using mesh-based generated reluctance networks," *IEEE Trans. Magn.*, vol. 54, no. 11, paper 7002304, Nov. 2018. DOI: 10.1109/TMAG.2018.282915
- [40] Boumedyen Nedjar, *Modélisation basée sur la méthode des réseaux de perméances en vue de l'optimisation de machines synchrones à simple et à double excitation*, Ph.D. Thesis Report, Ecole Normale Supérieure de Cachan, 2011 (in French). [Online]. Available @: <https://tel.archives-ouvertes.fr/tel-00675448/document>



Shuo Yang was born in Anhui, China, in 1995. He received the B.Sc. degree in electrical engineering and the M.Sc. degree from Southeast University, Nanjing, China, in 2017 and 2020, respectively.

His current research interests include the design, analysis, and control of permanent-magnet brushless electrical machines for application in electric

vehicles.



Salim Asfirane received the Ingénieur d'État degree in electrical engineering from École Nationale Polytechnique in Algiers, Algeria and the M.Sc. degree in electrical engineering from École Normale Supérieure de Cachan, France, in 2014 and 2015 respectively. In 2019, he finished his Ph. D. studies in Electrical Engineering in

Laboratoire des Systèmes et Applications des Technologies de l'Information et de l'Énergie (SATIE Laboratory) in collaboration with Groupe de Recherche en Électrotechnique et Automatique du Havre (GREAH

Laboratory) where he is currently pursuing his research. His interests include electromagnetic modeling methods and innovative design topologies of rotating and linear electrical machines.



Sami Hlioui received the electromechanical engineer diploma degree from the National School of Engineering of Sfax, Sfax, Tunisia, in 2004, the M.Sc. degree in electrical engineering from the Ecole Normale Supérieure de Cachan, Cachan, France, in 2005, and the Ph.D. degree in electrical power engineering from the University of

Technology of Belfort-Montbéliard, Belfort, France, in 2008. He is a Lecturer with the Conservatoire National des Arts et Métiers, Paris, France, and a Researcher with the Laboratory of Systems and Applications of Information and Energy Technologies, Ecole Normale Supérieure Paris-Saclay.

His main research interests include the multidisciplinary modeling of electromagnetic actuators and the optimal design of these actuators for embedded applications.



Smail Mezani received the Dipl.-Ing. and Magister degrees in electrical engineering from the University of Sciences and Technology, Houari Boumediene, Algiers, in 1996 and 1999, respectively, and the Ph.D. degree from the Institut National Polytechnique de Lorraine, Nancy, France, in 2004. He is assistant-professor of

Electrical Engineering with the Faculty of Sciences and Technology, University of Lorraine, Nancy, where his research works are undertaken in the Groupe de Recherche en Energie Electrique de Nancy Laboratory. His research interests include numerical and analytical modeling of electrical machines and contactless torque transmissions, coupled magnetic and thermal problems, and the applications of superconductors in electromechanical devices.



Guillaume Krebs was born in Croix, France, in 1978. He received the Engineering degree in 2003 and the Ph.D. degree in electrical engineering from the University Lille 1, Villeneuve-d'Ascq, France, in 2007. Since September 2008, he has been an Assistant Professor with the University of Paris-Sud,

Gif-sur-Yvette Cedex, France. His research interests (at the Paris Electrical and Electronic Engineering Laboratory) include the modeling and design of electrical machines by the finite-element method.



Yacine Amara (S'00–M'03–SM'18) received the Electrical Engineering Degree from Ecole Nationale Polytechnique d'Alger, El-Harrach, Algeria, in 1997, and the Ph.D. degree from the University of Paris XI, Orsay, France, in 2001. He is currently with the Groupe de Recherche en Electrotechnique et Automatique du Havre (GREAH),

University of Le Havre, Le Havre, France, where he holds a Full Professor position, and is heading the Electrical Machines and Actuators thematic. His research interests include the design, modeling, and control of rotating and linear permanent-magnet machines for automotive and renewable energies applications.



Georges Barakat received the M.Sc. and the Ph.D. degrees in Electrical Engineering from the Institut National Polytechnique de Grenoble, Grenoble, France, in 1992 and 1995, respectively. Currently, he is a Professor of Electrical engineering at University of Le Havre, where he is heading GREAH Group. His research interests include electrical

machines modeling, design and diagnosis



Mohamed Gabsi received the Ph.D. degree in electrical engineering from the University of Paris-VI, Paris, France, in 1987, and the HDR degree from the University of Paris-XI, Orsay, France, in 1999.

Since 1990, he has been working with the electrical machines team SETE of the Laboratory of Systems and Applications

of Information and Energy Technologies, Ecole Normale Supérieure Paris-Saclay, Saclay, France, where he is currently a Full Professor. His research interests include switched reluctance motor, vibrations and acoustic noise, and permanent magnet machines.



Wei Hua (M'03, SM'16) received the B.Sc. degree in Electrical Engineering from the Department of Electrical Engineering, Southeast University, Nanjing, China, in 2001, and the Ph.D. degree in Electrical Engineering from the School of Electrical and Electronic Engineering, Nanjing, China, in 2007.

During 2004.9-2005.8, he visited the Department of Electronics and Electrical Engineering, University of Sheffield, U.K., as a Joint-Supervised Ph. D. Student. Since 2007, he has been with Southeast University, where he is currently a Chief Professor with the School of Electrical Engineering. His teaching and research interests include design, analysis and control of electrical machines, especially for brushless machines, and motor drives for electric vehicles. He has authored or coauthored over 200 technical papers and is the holder of over 60 patents in these areas.